



Development and validation of a liquid chromatography coupled to tandem mass spectrometry method for the monitoring of temsavir plasma concentrations in people living with HIV

Paul Thoueille^{a,*}, Ulrich Seybold^b, Laurent A. Decosterd^a, Vincent Desfontaine^a

^a Service and Laboratory of Clinical Pharmacology, Department of Laboratory Medicine and Pathology, Lausanne University Hospital and University of Lausanne, Lausanne, Switzerland

^b Med. Klinik und Poliklinik IV, LMU Klinikum, Ludwig-Maximilians-University, Munich, Germany



ARTICLE INFO

Keywords:

Temsavir
Fostemsavir
LC-MS/MS
Therapeutic Drug Monitoring
HIV

ABSTRACT

A majority of people living with HIV (PLWH) now have access to HIV treatment with high antiviral potency and favorable tolerability profile. However, in some treatment experienced PLWH viral strains resistant to major current classes of antiretrovirals have emerged, usually due to periods with continued virus replication in the presence of failing drug regimens and thus selection pressure. In such context, new treatment options are therefore needed.

Fostemsavir (RUKOBIA®) is the prodrug of temsavir, a first-in-class oral attachment inhibitor approved for the treatment of heavily treatment-experienced adults with multidrug-resistant HIV-1 infection. In this case RUKOBIA® is part of a complex regimen of antiretroviral drugs, often in addition to other drugs for chronic comorbidities (e.g., heart disease, diabetes mellitus, hepatic and renal impairment, etc). In such a multi-drug regimen context, therapeutic drug monitoring (TDM) of temsavir can be necessary to exclude or adjust for relevant drug-drug interactions. A highly selective assay by liquid chromatography method coupled to tandem mass spectrometry (LC-MS/MS) was therefore developed for the quantification of temsavir in human plasma. A convenient sample preparation using protein precipitation with acetonitrile followed by supernatant dilution was carried out. Temsavir and fostemsavir were separated in less than 2 min using a multi-step UPLC gradient, thus ensuring adequate quantification of temsavir. The assay for the quantification of temsavir was extensively validated over the large range of clinically relevant concentrations from 1 to 10,000 ng/mL, in accordance with international bioanalytical method guidelines. The method achieves excellent performance in terms of trueness (99.7 – 105.3%), repeatability and intermediate precision (both from 1.6% to 5.8%).

This LC-MS/MS method is now part of the routine analyses of the Laboratory of the Service of Clinical Pharmacology of Lausanne (CHUV), Switzerland, as an integrated part of our general TDM Service for antiretrovirals.

1. Introduction

Over the past few decades, tens of millions people living with HIV (PLWH) have gained access to antiretroviral therapy (ART) transforming HIV infection from a deadly disease into a manageable chronic condition. In 2021, 28.7 million PLWH received ART globally, out of an estimated number of 38.4 million according to the World Health Organization [1].

Current guidelines for first-line antiretrovirals use in naïve PLWH recommend a potent HIV integrase strand transfer inhibitor *plus* two

nucleoside reverse transcriptase inhibitors (NRTI) or a non-nucleoside reverse transcriptase inhibitor *plus* two NRTI. However, in instances of ongoing virus replication in the presence of failing drug regimens the continuous selection pressure will eventually lead to the emergence of resistance mutations. Although this is less common than in the past thanks to more potent and effective treatments [2–4], some PLWH are confronted with viral strains resistant to major currently-in-use classes of antiretrovirals. In such instances of extensive HIV drug resistance, PLWH may be eligible to receive alternative combination regimens to ensure therapeutic effectiveness [5–8].

* Corresponding author.

E-mail address: Paul.Thoueille@chuv.ch (P. Thoueille).

<https://doi.org/10.1016/j.jchromb.2022.123575>

Received 11 November 2022; Received in revised form 8 December 2022; Accepted 8 December 2022

Available online 12 December 2022

1570-0232/© 2022 The Authors. Published by Elsevier B.V. This is an open access article under the CC BY license (<http://creativecommons.org/licenses/by/4.0/>).

Fostemsavir (Rukobia®) is the prodrug of temsavir, a first-in-class oral attachment inhibitor that binds directly to HIV-1 gp120, preventing the virus from initially attaching and entering host CD4+ T cells [9]. Fostemsavir is not absorbed but requires enzymatic conversion to temsavir by alkaline phosphatase present in the gastrointestinal lumen [10]. Temsavir is a substrate of cytochrome P450 3A4, P-glycoprotein, and breast cancer resistance protein (BCRP). Temsavir is *per se* also an inhibitor of BCRP and of the organic anion transporter protein OATP1B1/3 [11,12]. Thus, temsavir may be at risk of significant reciprocal drug-drug interactions. In particular, it is contraindicated in combination with strong CYP3A4 inducers, which would decrease plasma levels, hence leading possibly to therapeutic failure [13]. Yet, as it has been designed to inhibit an alternate viral target, fostemsavir constitutes a novel practical option in combination with optimized background antiretroviral therapy, for heavily treatment-experienced adults with multidrug-resistant HIV-1 infection. The 600 mg twice-daily extended release formulation was approved by the U.S. FDA in 2020, and by Swissmedic in 2021 [13–15]. In the frequently complex clinical situation of heavily treatment-experienced patients with multidrug-resistant HIV-1 infection, physicians may seek information on temsavir exposure to ensure adequate plasma concentration levels in these PLWH. In particular, therapeutic drug monitoring (TDM) may be advised when suboptimal adherence is suspected or when drug absorption may be impaired.

The present article describes, to the best of our knowledge, the first completely validated ultra-performance liquid chromatography coupled to tandem mass spectrometry (LC-MS/MS) method for the quantification of temsavir (the active species of the prodrug fostemsavir) in human plasma.

2. Materials and methods

2.1. Chemicals and reagents

Fostemsavir (purity $\geq 98\%$), temsavir (purity $\geq 98\%$) and the stable isotopically-labelled internal standard (IS) [$^{13}\text{C}_6$]-Temsavir (purity $\geq 99.7\%$; isotopic purity: $M + 6 = 97.8\%$, $M + 5 = 2.2\%$) were generous gifts from GlaxoSmithKline (Brentford, Middlesex, UK) through ViiV Healthcare. Of note, the ^{13}C isotopes are located on the benzylpiperazine group. Chemical structures are shown in Fig. 1.

Analytical solvents (i.e. methanol (MeOH, analysis grade), acetonitrile (ACN, gradient grade), and formic acid (FA, 98–100%)) were purchased from Merck (Darmstadt, Germany). Dimethylsulfoxide (DMSO, 99.5%) was obtained from Alfa Aesar (Kandel, Germany), and ultrapure water was provided by a Milli-Q UF-Plus apparatus (Millipore Corp, Burlington, MA, USA).

In accordance with the institutional ethical standard, human blood samples used for all steps of the method development and validation

were obtained from patients with *polycythemia vera* undergoing regular phlebotomies at the Ambulatory Care Unit, Unisanté, University of Lausanne, Switzerland. After collection of the citrated blood plasma samples, blank plasma was separated by centrifugation (1970 g for 10 min at +4 °C) using a Hettich model Rotanta 460RF centrifuge.

2.2. Stock solutions preparation

Analytes (temsavir and fostemsavir) stock solutions were prepared at 2 mg/mL in DMSO and subsequently stored at $-20\text{ }^\circ\text{C}$.

Independent working solution (WS) of temsavir at 200 $\mu\text{g/mL}$ was prepared in a mixture of ACN:H₂O (3:1) for calibration and validation standards. Then, sequential dilutions of the WS in ACN:H₂O (3:1) were performed to obtain spiking solutions at the appropriate concentrations.

The stock solution of [$^{13}\text{C}_6$]-Temsavir was prepared at 1 mg/mL in DMSO, from which a precipitation solution was prepared at 250 ng/mL by diluting the stock solution with ACN. These solutions were stored at $-20\text{ }^\circ\text{C}$.

2.3. Calibration and validation standards

In the present method, the quantification of the prodrug fostemsavir was not considered but fostemsavir was nevertheless included at the initial stage of the analytical development for ascertaining that fostemsavir was sufficiently separated chromatographically from the active species temsavir, to exclude any risk of *m/z* signal cross-talks that would spuriously affect temsavir assay accuracy. In accordance to the recommendations for bioanalytical method validation [16,17], the total added volume of spiking solutions was $\leq 10\%$ of the biological sample volume. Spiked plasma was obtained by diluting the spiking solutions (25 μL) 20-fold with blank plasma (475 μL). Calibration standards were prepared on each validation day ($n = 3$) at the following eight concentration levels: 10,000, 4000, 1000, 500, 125, 25, 5, and 1 ng/mL with respect to the clinically relevant concentrations reported in clinical trials [13,14]. In addition, five validation standards were prepared at the following concentrations: 10,000, 1000, 100, 10, and 1 ng/mL.

2.4. Plasma treatment procedure

A convenient protein precipitation step was performed by mixing a 50- μL aliquot of calibration or validation standards with 150 μL of the precipitation solution. The mixture was then vortexed and centrifuged following a standardized procedure (18,620g for 10 min at +4 °C) using a Benchtop Mikro 220R centrifuge (Hettich, Bäch, Switzerland). The supernatant was finally diluted 1:1 with fresh MilliQ water (100 μL precipitated plasma + 100 μL H₂O into an HPLC vial with insert).

Plasma samples from patients receiving fostemsavir (Rukobia®) as part of their multiple antiretroviral regimens were analyzed with the developed LC-MS/MS method as a quality control within the frame of the hospital routine antiretroviral TDM program. According to Swiss Law and Institutional rules, ethical approval is not required for a retrospective case report involving anonymised clinical data (see the Federal Act on Research involving Human Beings [18]).

2.5. LC-MS/MS instrumentation

LC-MS/MS analyses were performed using a Vanquish Flex ultra-high-performance liquid chromatography system (ThermoFisher Scientific, San Jose, CA, USA), equipped with a 2-channel binary high-pressure gradient pump limited to 15,000 psi (1000 bar), a thermostated flow-through needle auto-sampler with temperature range between 4 °C and 40 °C, and a column oven with temperature range between 5 °C and 120 °C. Chromatographic separation was conducted with a Luna® Omega Polar C18 analytical column from Phenomenex (Torrance, CA, USA) with 3 μm particle size and dimensions of 50 \times 2.1 mm. The chromatographic system was coupled to a TSQ Quantis triple

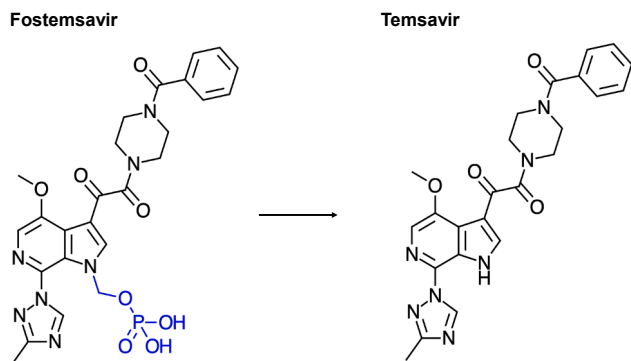


Fig. 1. Chemical structures of temsavir and its prodrug fostemsavir. In blue, the phosphonoxyethyl group lost during hydrolysis of fostemsavir yielding to the active substance temsavir.

quadrupole mass spectrometer from Thermo Fisher Scientific, equipped with an OptaMax NG ion source used in electrospray ionization (H-ESI) mode. Data acquisition and processing, as well as instrument control, were performed using the XCalibur software version 4.1.31.9 and Chromeleon version DCMS link (ThermoFisher Scientific).

2.6. Analytic conditions

The mobile phases (i.e. H₂O + 0.1% FA (A) and ACN + 0.1% FA (B)) were delivered at flow rate of 0.5 mL/min using the following multi-step gradient: linear gradient from 10 to 60% B in 1.5 min, up to 95% B in 0.3 min, followed by an isocratic stage at 95% B for 0.7 min, and a re-equilibration step at 10% B during 1.5 min (total analysis time of 4 min). The injection volume was 4 μ L, and samples were stored at +5 °C in the auto-sampler.

ESI source parameters were optimized as follows: vaporizer and ion transfer tube temperatures were both set at 350 °C, and sheath, auxiliary, and sweep gas flow rates at 65, 20, and 0 (arbitrary units), respectively. The mass resolutions used to operate the first (Q1) and third (Q3) quadrupoles were 0.7 and 1.2 Da, respectively. In the second quadrupole (Q2), the pressure of the collision gas (argon) was set at 2 mTorr. Lastly, the capillary voltage was 3000 V and cycle time was 0.15 s.

2.7. Validation procedure

2.7.1. Selectivity, cross-talk, and carryover

The selectivity of the method was first established by the analysis of blank human plasma obtained from 10 different donors (seven regular and three lipemic), processed with pure ACN. Subsequently, a blank human plasma processed with IS and the highest calibration standard processed with pure ACN were analyzed to identify potential interferences between temsavir and its IS due to the MS-based cross-talk phenomenon. Moreover, carryover was assessed by injecting a processed blank plasma immediately after the highest calibration processed with IS.

In addition, the LC gradient was optimized to ensure an optimal chromatographic separation of temsavir from the prodrug fostemsavir, which differs by one phosphonoxyethyl group (see Fig. 1).

2.7.2. Qualitative evaluation of matrix effect

Matrix effect was qualitatively assessed according to the method proposed by Bonfiglio *et al.* [19], which allows the evaluation of the impact of endogenous compounds on the ionization process. A temsavir solution at 100 ng/mL in ACN:H₂O (3:1) was directly infused post-column while ten different blank plasma samples (seven regular and three lipemic) processed with pure ACN were injected using the LC-MS/MS method described earlier. The resulting chromatographic profiles were visually inspected for potential matrix interference at the analyte and IS retention time.

2.7.3. Quantitative evaluation of matrix effect, extraction recovery, and process efficiency

Matrix effect (ME), extraction recovery (ER), and process efficiency (PE) were quantitatively evaluated following the approach proposed by Matuszewska *et al.* [20]. Sets of samples at low (20 ng/mL), medium (200 ng/mL), and high (2000 ng/mL) concentrations were prepared: (A) neat solutions of ACN:H₂O (37.5:62.5) with temsavir and its IS (in triplicates); (B) ten post-extraction spiked blank plasma; (C) ten pre-extraction spiked blank plasma. For each set of samples, the average analyte to IS peak area ratio was monitored and, subsequently, normalized matrix effect (*n*-ME) as B/A (%), normalized extraction recovery (*n*-ER) as C/B (%), and normalized process efficiency (*n*-PE) as C/A (%) were calculated.

2.7.4. Trueness, precision, accuracy profile, limits of quantification, and linearity

The determination of the intra- and inter-assay accuracy and precision values was performed at five concentration levels in triplicate over three different days. The optimal quantitative relationship between response and concentration was determined by back-calculating the concentrations of the validation standards using daily calibration curves constructed with different mathematical regression models. The bias between the nominal and measured concentrations was used to determine trueness (systematic error). The precision parameters, i.e. repeatability (intra-day variance) and intermediate precision (intra-day and inter-day variances), were also calculated [21–23], and reported as relative standard deviation (RSD) at each concentration level [24]. The total error, which encompasses both systematic and random errors, was evaluated thanks to the establishment of accuracy profiles, using β -expectation tolerance intervals (i.e. the concentration range in which $\beta\%$ of future results are expected) [25–27]. Typically, the lower limit of quantification (LLOQ) is graphically interpolated on the basis of the absolute accuracy profiles, and it is defined as the lowest concentration for which the β -expectation tolerance interval crosses the acceptance limits ($\pm 30\%$) [16,17,28]. In the present case, the LLOQ was also chosen based on the relevance for routine assays. On the other hand, the limit of detection (LOD) of the method was assessed by injecting processed plasma samples spiked with different concentrations below 1 ng/mL. The chromatograms were visually examined to determine the LOD values.

Finally, the estimations of trueness and precision, the narrowest β -expectation tolerance interval, and the lowest LLOQ enabled the selection of the best calibration model [24]. In addition, ordinary least squares regression of back-calculated concentrations versus nominal concentrations for validation standards was used to assess the capacity of the method to give proportional quantitative results.

2.7.5. Measurement uncertainty

The measurement uncertainty (MU) represents the range of possible values of the result and can be calculated, notably, from the type A estimation method, which is based on the statistical distribution of experimental measurements. As demonstrated by Feinberg *et al.* [29], MU can be computed from the β -expectation tolerance interval without any additional experiments. Therefore, by exploiting the accuracy profile validation methodology, it is then possible to estimate MU directly by setting the β value at 0.95 [30]. Several continuous models were developed, and the resulting uncertainty profiles were visually inspected to identify the one best fitting the data. MU values could then be generated as a function of analyte concentration, allowing the MU to be easily calculated at any concentration within the validation domain.

2.7.6. Stability studies

The stability of temsavir in plasma and in whole blood at low and high concentrations (i.e. 100 and 1500 ng/mL, respectively) was evaluated at room temperature (RT) and at 4 °C up to 72 h. In addition, stability after three freeze–thaw cycles (1-hour freezing at –80 °C and –20 °C and thawing at room temperature) was assessed with plasma samples. Finally, medium term stability was assessed with plasma samples frozen at –80 °C during 7 weeks. All the analyses were performed in triplicate and the average concentrations obtained for each time point was compared with the average concentration of samples prepared at t_0 .

Despite that plasma concentrations of fostemsavir were found to be undetectable, thus confirming presystemic conversion to temsavir [13,31], we still examined the stability of fostemsavir in plasma and whole blood at RT, to fully exclude any *ex vivo* conversion to temsavir (see Fig. 1).

2.7.7. Clinical application

Blood samples were collected in EDTA from PLWH during the usual

follow-up visits. After centrifugation of the EDTA blood plasma was transferred into propylene tubes in class II biohazard hoods using standard biosafety precautions. Samples were stored at -20°C until analysis.

3. Results and discussion

3.1. Analytical method development

Optimal precursor and product ions spectra were determined in ESI+ mode by performing direct MS infusion at $10\ \mu\text{L}/\text{min}$ of a solution of temsavir at $5\ \mu\text{g}/\text{mL}$ in MeOH. The most abundant precursor ion was, not unexpectedly, the one corresponding to $[\text{M} + \text{H}]^{+}$ at m/z 474 Da. The three most abundant product ions were identified and selected, and the three corresponding MRM transitions were summed to enhance the sensitivity during quantification ($474 > 104.9$, $474 > 214.9$ and $474 > 256$). No comparison could be made with the literature since no LC-MS/MS method has been reported yet for the determination of temsavir in plasma. Optimized MS/MS parameters are reported in Table 1.

In order to avoid spuriously high levels of temsavir resulting from possible source-induced hydrolysis of fostemsavir during the ionization step (although unlikely, see comment above in Section 2.7.6), chromatographic conditions were optimized to achieve satisfactory separation between temsavir and its prodrug fostemsavir. Conventional mobile ($\text{H}_2\text{O} + 0.1\% \text{FA}$ and $\text{ACN} + 0.1\% \text{FA}$) and stationary (Luna® Omega Polar C18 column) phases were found to give appropriate retention and peak shapes. Mobile phase gradient program was then optimized to minimize the run time and improve separation. Fig. 2 shows the LC separation of fostemsavir and temsavir.

A standard, convenient and fast protein precipitation was selected for the sample treatment. The sensitivity of the method was compared when using different solvents for the protein precipitation (MeOH and ACN). ACN turned out to be the best alternative. In order to improve peak shapes, the supernatant arising from the processed plasma was diluted 2-fold with milliQ H_2O prior to LC-MS/MS injection. With such a dilution, the injection volume could be increased up to $4\ \mu\text{L}$, allowing the best compromise between sensitivity and peak shape.

The MS conditions were optimized by adjusting the ESI source

Table 1

MS/MS parameters and typical retention times of temsavir, its prodrug fostemsavir and the stable isotopically-labelled IS [$^{13}\text{C}_6$]-Temsavir.

Compound	ESI polarity (+/-)	Precursor Ion (m/z)	Product Ion (m/z)	Collision Energy (eV)	RF Lens (V)	Retention time (min)
Fostemsavir	+	584.1	104.9	43	136	1.49
			268.0	42		
			486.0	18		
Temsavir	+	474.0	104.9	24	148	1.91
			214.9	38		
			256.0	22		
[$^{13}\text{C}_6$]-Temsavir	+	480.0	110.9	24	149	1.91
			214.9	38		
			256.0	22		

ESI: Electrospray Ionization.

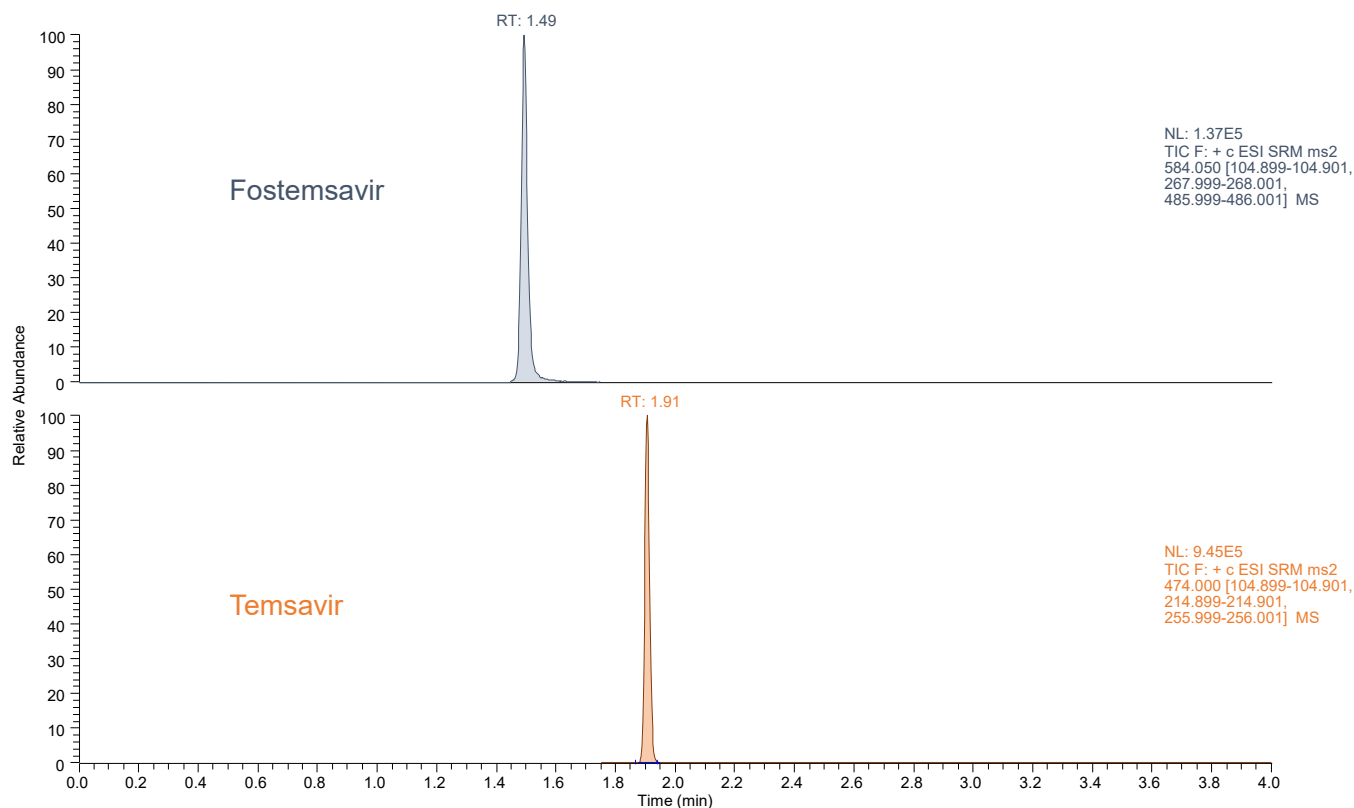


Fig. 2. Chromatographic profiles showing the separation of temsavir and its prodrug fostemsavir as synthetic standards in a solution of ACN:H₂O (3:1) at the concentration of 2000 ng/mL.

parameters to obtain the best signal to noise ratio (i.e. minimizing background noise while improving signal sensitivity). In order to obtain satisfactory IS-normalized response functions, the concentration of [$^{13}\text{C}_6$]-Temsavir was adjusted. An intermediate concentration of 250 ng/mL in the precipitation solution was selected in order to avoid excessive variability at lower concentrations and potential significant contribution of the residual unlabeled IS to the analyte signal at higher concentrations.

3.2. Validation of the method

3.2.1. Selectivity, cross-talk, and carryover

The analyses of the ten different blank plasmas demonstrated good selectivity of the chromatographic method, with no significant matrix interference observed at the retention time of temsavir. In addition, no relevant cross-talk interference between temsavir and its IS was observed when inspecting the chromatographic profiles corresponding to the injections of a blank human plasma processed with the precipitation solution (containing the IS) and the highest calibration concentration (10,000 ng/mL) processed with pure ACN. Finally, carryover experiments revealed a signal at 32% of the LLOQ (injection of a blank plasma after the calibration standard with highest concentration). The

FDA recommendations (carryover of less than 20% of LLOQ) were finally fulfilled by adding an injection of blank MeOH in between the highest calibration samples and the first sample of the analytical series constituted by blank human plasma.

3.2.2. Matrix effect, extraction recovery, and process efficiency

Fig. 3 shows that no major interference, i.e. ion suppression or enhancement, was observed at the retention time of temsavir, thus confirming the suitability of the chromatographic method. The major signal alterations were observed at retention times between 0.2 and 0.3 min (total ion suppression due to elution of polar compounds from plasma) and between 2.4 and 2.8 min (strong ion suppression due to elution of phospholipids from plasma).

On the other hand, Table 2 presents the quantitative results of the evaluation of *n*-ME, *n*-ER and *n*-PE. All the values were comprised between 80 and 120% for all the concentrations levels, with RSD values lower than 15%. In conclusion, the IS was well adapted to correct (if needed) the signal variability due to interferences from the processed plasma and the potential loss of analyte during the sample treatment.

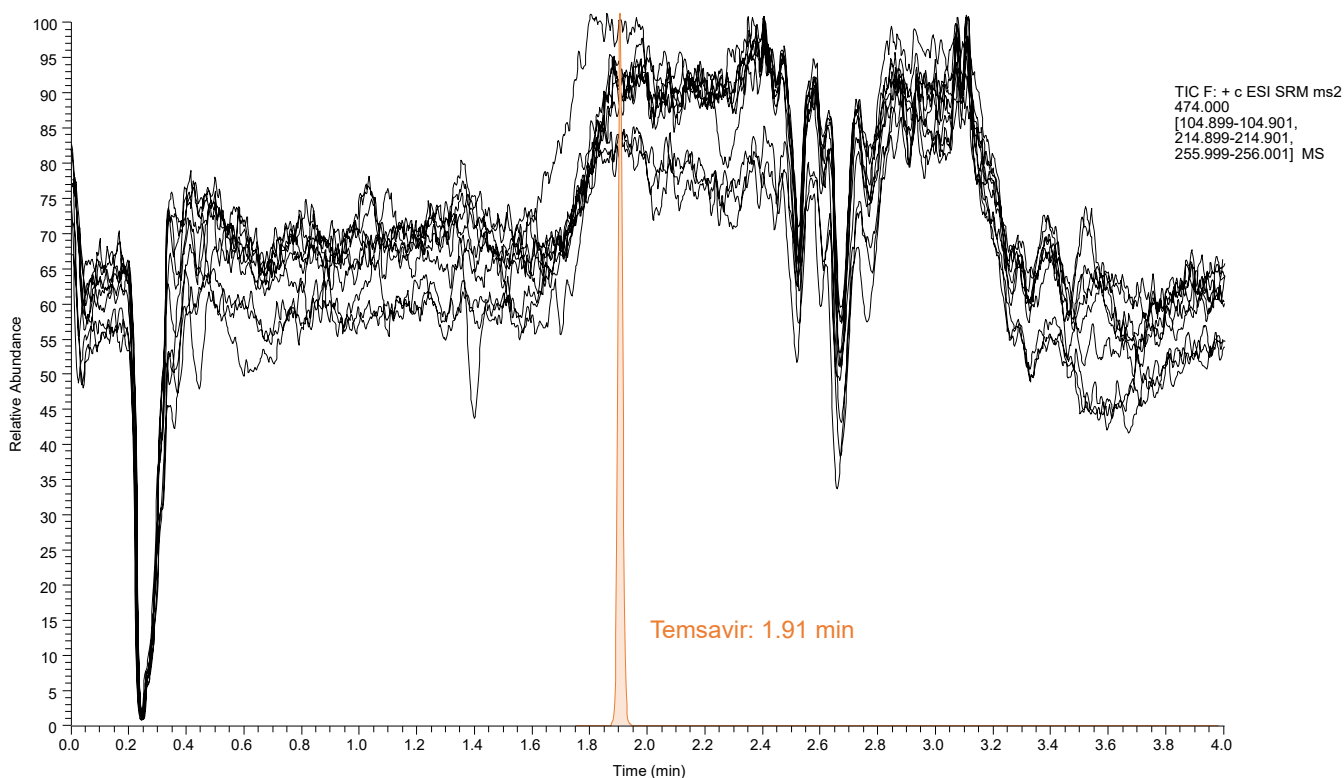


Fig. 3. Qualitative evaluation of matrix effect in human plasma. Overlaid LC-MS/MS profiles were obtained from the injections of ten different blank plasma samples (including 3 lipemic plasmas) processed with pure ACN, during post-column infusion of temsavir at 100 ng/mL in ACN:H₂O (3:1). Temsavir peak obtained with the developed method was overlaid for interpretation.

Table 2

Internal standard-normalized matrix effect (*n*-ME), extraction recovery (*n*-ER), and process efficiency (*n*-PE) for temsavir (average value calculated from 10 different human plasmas).

	Concentration (ng/mL)	<i>n</i> ME		<i>n</i> ER		<i>n</i> PE	
		%	RSD (%)	%	RSD (%)	%	RSD (%)
Temsavir/[$^{13}\text{C}_6$]-Temsavir	20	97	6	112	6	108	2
	200	98	9	116	2	114	2
	2000	101	8	113	7	114	2

RSD: relative standard deviation.

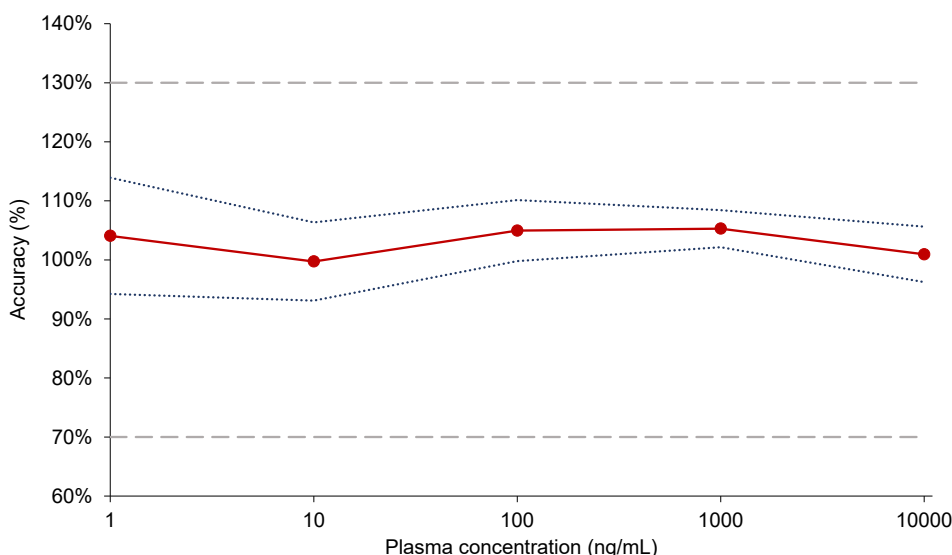


Fig. 4. Accuracy profile over the considered validation domain of temsavir in human plasma (five concentration levels in triplicate over three different days). Trueness (red solid line), upper and lower β -expectation tolerance intervals ($\beta = 90\%$) (blue dotted lines) and acceptance limits ($\lambda = \pm 30\%$), beige dotted lines) are shown.

3.2.3. Trueness, precision, accuracy profile, limits of quantification, and linearity

The quadratic log-log regression model provided the best response function (i.e. temsavir/IS peak area ratio in function of temsavir concentrations) in terms of determination coefficient and back-calculated calibration samples ($\pm 15\%$). Validation standards of temsavir, calculated using the calibration curves, ranged from 1 to 10,000 ng/mL. At all validation sample concentrations examined, the trueness was comprised between 100% and 106%, while the repeatability (i.e. within-run precision) and the intermediate fidelity (i.e. between-run precision) ranged from 1.6% to 5.8%, respectively, and were therefore considered appropriate for the quantification of temsavir plasma levels.

The β -expectation tolerance intervals (i.e. fraction of future results that are expected to fall within the tolerance intervals obtained in the routine application of the method [32]) were generated by setting the β value to 90%. Fig. 4 shows the accuracy profile generated from the data obtained during the three days of method validation. For all validation concentration levels, the β -expectation tolerance intervals are encompassed within the acceptance limits of $\pm 30\%$ for biological samples [17]. Therefore, the LLOQ and the upper limit of quantification (ULOQ)

were defined as the lowest and highest concentrations of validation sample, i.e. 1 ng/mL and 10,000 ng/mL, respectively. It was observed that temsavir could be reliably detected at 100 pg/mL, and thus possibly quantified at lower concentrations than 1 ng/mL. However, it did not seem relevant for clinical applications to try to reduce the LLOQ.

Finally, linearity turned out to be satisfactory since determination coefficients (R^2) values were above 0.999 for the three days of validation.

3.2.4. Measurement uncertainty

A polynomial regression model best described the absolute uncertainty vs concentration profile, with an R^2 of 1. As shown in Table 3, the relative uncertainty is higher at low concentrations of the validation domain, reaching a maximum of 14% for the LLOQ.

3.2.5. Stability studies

Results for stability studies, reported in Table 4, show that temsavir is stable in plasma and whole blood samples at RT and +4 °C for at least 72 h. In addition, the three consecutive freeze-thaw cycles did not affect plasma concentrations. Finally, the medium-term stability studies

Table 3
Accuracy and precision values for the method validation of temsavir in human plasma, as well as the estimation of relative uncertainty.

	Concentration (ng/mL)	Trueness (%)	Precision		Relative uncertainty (%)
			Repeatability (%)	Intermediate precision (%)	
Temsavir	1	104.1	5.8	5.8	14
	10	99.7	2.6	3.8	11
	100	105.0	2.6	2.6	6
	1000	105.3	1.6	1.6	4
	10,000	100.9	2.1	2.6	7

Table 4
Stability studies.

Compound	Concentration (ng/mL)	Plasma		Whole blood		After 3 consecutive freeze-thaw cycles		Stability of plasma samples over 7 weeks
		RT for 72 h	+4°C for 72 h	RT for 72 h	+4°C for 72 h	At -20 °C	At -80 °C	
Temsavir	100	1%	2%	-6%	-1%	1%	2%	-5%
	1500	2%	1%	-7%	-3%	0%	-1%	13%

RT: room temperature.
Data are reported as deviations from concentration measured at t_0 .

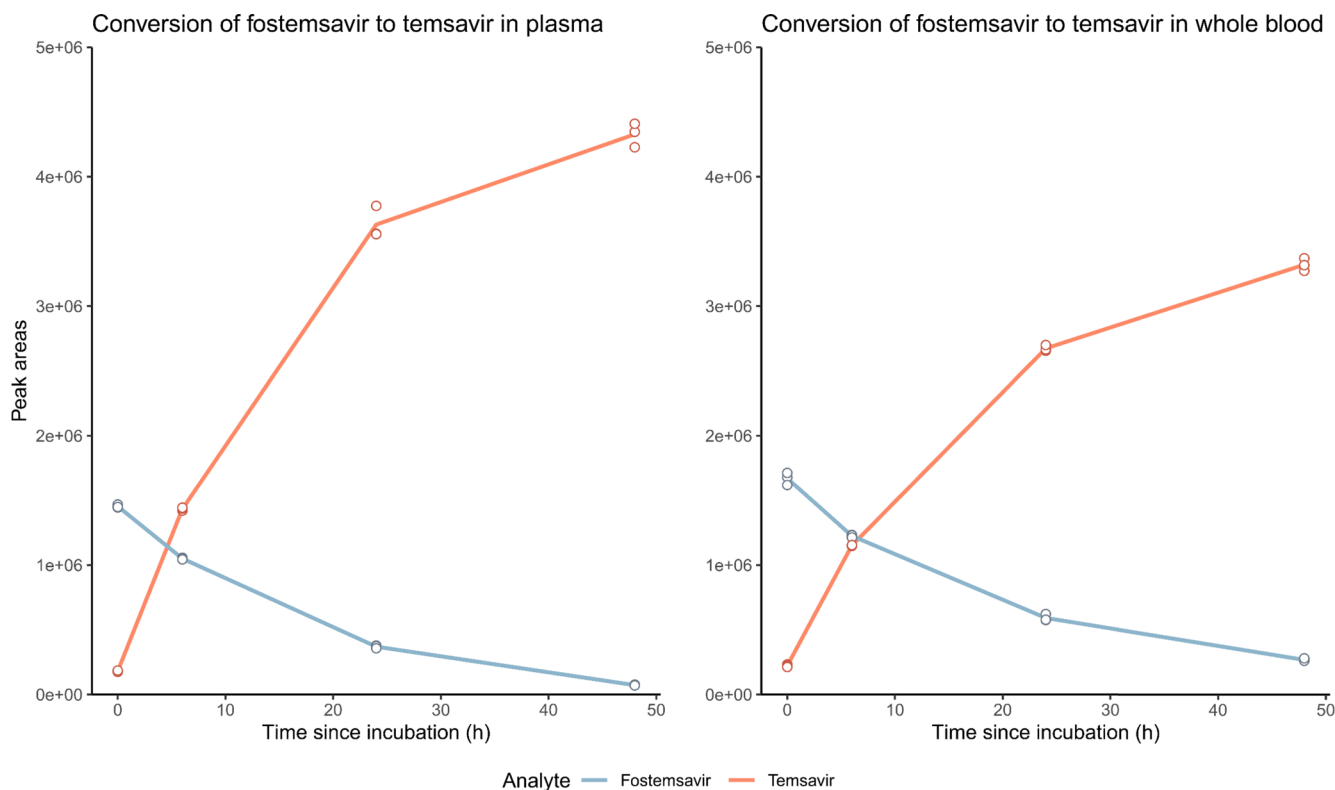


Fig. 5. Conversion of fostemsavir to temsavir in plasma (left panel) and in whole blood (right panel) after incubation of fostemsavir at 2000 ng/mL at room temperature. The analyses were performed in triplicate (points) and mean values were represented with lines.

demonstrated that temsavir plasma samples were not altered after 7 weeks of freezing at -80°C . Fig. 5 illustrates the conversion of fostemsavir into temsavir in plasma and in whole blood. The results show that there is a rapid conversion of fostemsavir to temsavir *ex vivo*. Nevertheless, fostemsavir is not expected to be found in blood samples collected from PLWH as the conversion to temsavir is presystemic [13,31].

3.3. Clinical application

Fig. 6 shows an example of LC-MS/MS profile of a plasma sample collected from a PLWH receiving Rukobia® 2 times a day on the top of an antiretroviral regimen consisting of dolutegravir twice daily, lamivudine once daily, and ibalizumab injected intravenously every-two weeks. The method was also applied for temsavir quantification in a plasma from another PLWH receiving Rukobia® twice daily in addition to dolutegravir twice daily and emtricitabine every 96 h. Both of these patients are also receiving multiple medications for their co-morbidities. Temsavir plasma concentrations in these patients were 391 ng/mL and 504 ng/mL, 15 h and 7 h after the intake of fostemsavir, respectively. These concentrations are in line with reported data [33,34].

As expected, the signal of the pro-drug fostemsavir which is monitored in parallel at m/z transition $584.1 > 486.0$, $584.1 > 268.0$ and $584.1 > 104.9$ is not observed. No other peaks were found, despite a very complex multiple drugs regimen, demonstrating again the exquisite selectivity of the LC-MS/MS approach.

4. Conclusion

A sensitive LC-MS/MS method for the quantification of temsavir in human plasma was developed and validated. International recommendations for bioanalytical determination were fulfilled over a large concentration range to cover the plasma levels of temsavir reported so far in clinical trials. The method has been included to the routine analyses of

the Laboratory of Clinical Pharmacology of Lausanne University Hospital (CHUV), Switzerland. As an integrated part of our routine therapeutic drug monitoring service for antiretrovirals, this method offers the opportunity to perform in-depth pharmacokinetic studies of temsavir in heavily treatment-experienced patients, possibly improving patient care.

Funding

This work was supported by the Swiss National Science Foundation, Grant No N° 324730_192449 (to L.A.D).

CRediT authorship contribution statement

Paul Thoueille: Conceptualization, Formal analysis, Investigation, Methodology, Visualization, Writing – original draft. **Ulrich Seybold:** Supervision, Data curation, Investigation, Writing – review & editing. **Laurent A. Decosterd:** Conceptualization, Funding acquisition, Project administration, Resources, Supervision, Validation, Writing – review & editing. **Vincent Desfontaine:** Conceptualization, Supervision, Validation, Writing – review & editing.

Declaration of Competing Interest

The authors declare that they have no known competing financial interests or personal relationships that could have appeared to influence the work reported in this paper.

Data availability

The data that has been used is confidential.

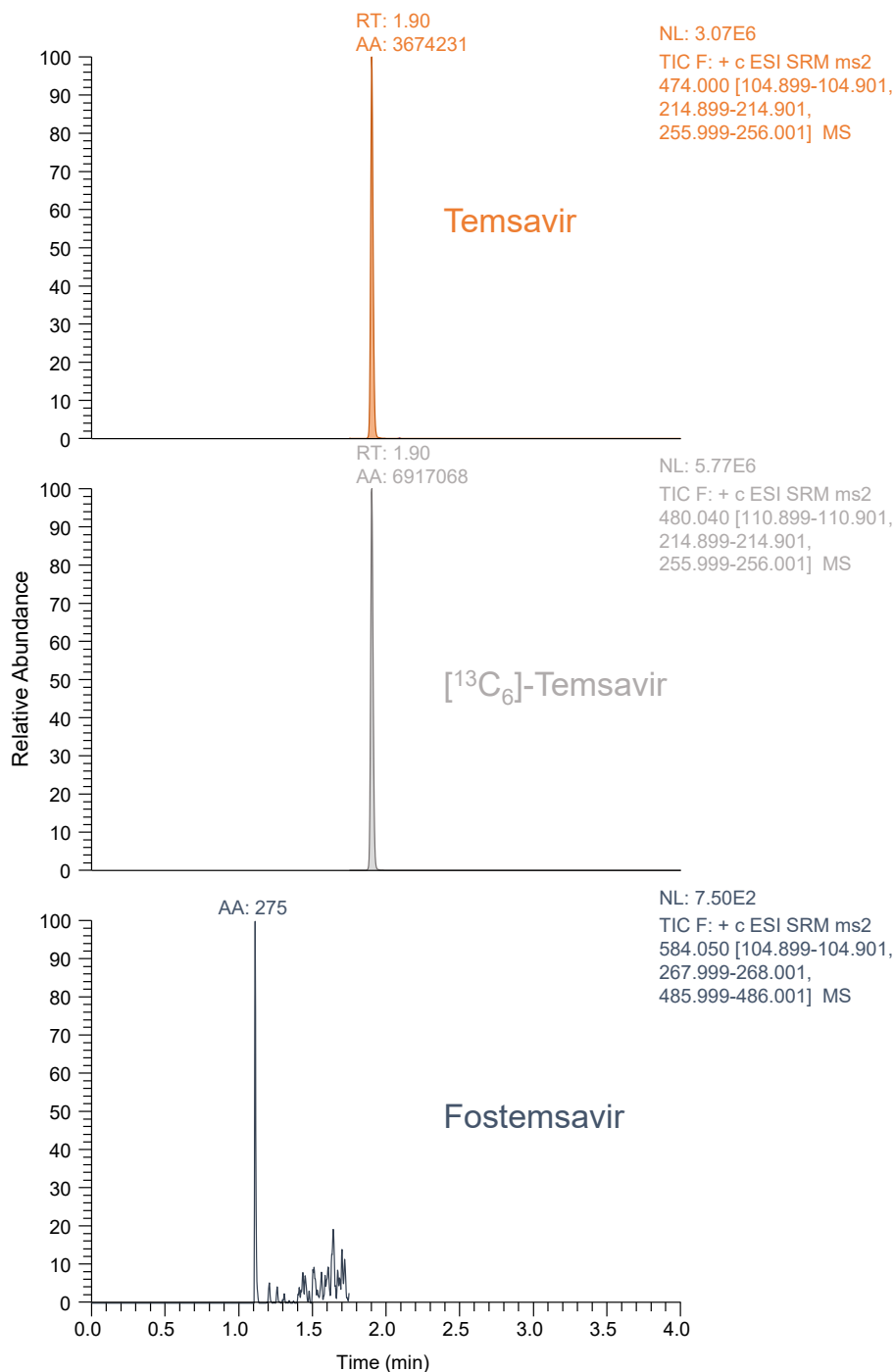


Fig. 6. LC-MS/MS profile of a human plasma sample collected from a PLWH receiving Rukobia® 2 times a day as part of an antiretroviral salvage-regimen that also included lamivudine once per day, dolutegravir twice per day, and ibalizumab every 2 weeks.

Acknowledgment

The authors would like to thank Stéphane Charbon (ViiV Healthcare) for providing the necessary standards (Fostemsavir and temsavir pure substances, and the stable isotopically-labelled internal standard [$^{13}\text{C}_6$]-Temsavir) for initial method's development. We are also indebted to Ilse Ott, for her invaluable help in patient samples' logistics.

References

- [1] World Health Organization (WHO). HIV Key facts. <https://www.who.int/news-room/fact-sheets/detail/hiv-aids> (accessed 25 October 2022).
- [2] L. Assoumou, C. Charpentier, P. Recordon-Pinson, M. Grudé, C. Pallier, L. Morand-Joubert, S. Fafi-Kremer, A. Krivine, B. Montes, V. Ferré, M. Bouvier-Alias, J. C. Plantier, J. Izopet, M.A. Traub, S. Yerly, J. Dufayard, C. Alloui, L. Courdavault, H. Le Guillou-Guillemette, A. Maillard, C. Amiel, A. Vabret, C. Roussel, S. Vallet, J. Guinard, A. Mirand, A. Beby-Defaux, F. Barin, A. Allardet-Servent, R. Ait-Namane, M. Wirten, C. Delaugerre, V. Calvez, M.L. Chaix, D. Descamps, S. Reigadas, Prevalence of HIV-1 drug resistance in treated patients with viral load >50 copies, mL: a 2014 French nationwide study, *J. Antimicrob. Chemother.* 72 (2017) 1769–1773, <https://doi.org/10.1093/jac/dkx042>.
- [3] G. Rocheleau, C.J. Brumme, J. Shoveller, V.D. Lima, P.R. Harrigan, Longitudinal trends of HIV drug resistance in a large Canadian cohort, 1996–2016, *Clin. Microbiol. Infect.* 24 (2018) 185–191, <https://doi.org/10.1016/j.cmi.2017.06.014>.
- [4] A.U. Scherrer, V. von Wyl, W.L. Yang, R.D. Kouyos, J. Böni, S. Yerly, T. Klimkait, V. Aubert, M. Cavassini, M. Battegay, H. Furrer, A. Calmy, P. Vernazza, E. Bernasconi, H.F. Günthard, V. Aubert, M. Battegay, E. Bernasconi, J. Böni, D.

- L. Braun, H.C. Bucher, C. Burton-Jeangros, A. Calmy, M. Cavassini, G. Dollenmaier, M. Egger, L. Elzi, J. Fehr, J. Fellay, H. Furrer, C.A. Fux, M. Gorgievski, H. Günthard, D. Haerry, B. Hasse, H.H. Hirsch, M. Hoffmann, I. Hösl, C. Kahlert, L. Kaiser, O. Keiser, T. Klimkait, R. Kouyos, H. Kovari, B. Ledergerber, G. Martinetti, B. Martinez de Tejada, C. Marzolini, K. Metzner, N. Müller, D. Nadal, D. Nicca, G. Pantaleo, A. Rauch, S. Regenass, C. Rudin, F. Schöni-Affolter, P. Schmid, R. Speck, M. Stöckle, P. Tarr, A. Trkola, P. Vernazza, R. Weber, S. Yerly, Emergence of Acquired HIV-1 Drug Resistance Almost Stopped in Switzerland: A 15-Year Prospective Cohort Analysis, *Clin. Infect. Dis.* 62 (2016) 1310–1317, <https://doi.org/10.1093/cid/ciw128>.
- [5] J.M. Llibre, C.C. Hung, C. Brinson, F. Castelli, P.M. Girard, L.P. Kahl, E.A. Blair, K. Angelis, B. Wynne, K. Vandermeulen, M. Underwood, K. Smith, M. Gartland, M. Aboud, Efficacy, safety, and tolerability of dolutegravir-ripivirine for the maintenance of virological suppression in adults with HIV-1: phase 3, randomised, non-inferiority SWORD-1 and SWORD-2 studies, *Lancet (London, England)* 391 (2018) 839–849, [https://doi.org/10.1016/S0140-6736\(17\)33095-7](https://doi.org/10.1016/S0140-6736(17)33095-7).
- [6] D. Sculier, G. Wandeler, S. Yerly, A. Marinosci, M. Stoeckle, E. Bernasconi, D. L. Braun, P. Vernazza, M. Cavassini, M. Buzzi, K.J. Metzner, L.A. Decosterd, H. F. Günthard, P. Schmid, A. Limacher, M. Egger, A. Calmy, M.-L. Newell, Efficacy and safety of dolutegravir plus emtricitabine versus standard ART for the maintenance of HIV-1 suppression: 48-week results of the factorial, randomized, non-inferiority SIMPL'HIV trial, *PLoS Med.* 17 (11) (2020) e1003421.
- [7] C. Katlama, J. Ghosn, G. Wandeler, VIH Hépatites virales Santé sexuelle, *EDP Sci.* (2020).
- [8] European AIDS Clinical Society (EACS) Guidelines. Version 11.1. October 2022.
- [9] M.C. Cambou, R.J. Landovitz, Novel Antiretroviral Agents, *Curr. HIV/AIDS Rep.* 17 (2020) 118–124, <https://doi.org/10.1007/s11904-020-00486-2>.
- [10] J. Brown, C. Chien, P. Timmins, A. Dennis, W. Doll, E. Sandefer, R. Page, R. E. Nettles, L. Zhu, D. Grasela, Compartmental absorption modeling and site of absorption studies to determine feasibility of an extended-release formulation of an HIV-1 attachment inhibitor phosphate ester prodrug, *J. Pharm. Sci.* 102 (2013) 1742–1751, <https://doi.org/10.1002/jps.23476>.
- [11] M. Berruti, R. Pincino, L. Taramasso, A. Di Biagio, Evaluating fostemsavir as a therapeutic option for patients with HIV, *Expert Opin. Pharmacother.* 22 (2021) 1539–1545, <https://doi.org/10.1080/14656566.2021.1937120>.
- [12] N. Seval, C. Frank, M. Kozal, Fostemsavir for the treatment of HIV, *Expert Rev. Anti Infect. Ther.* 19 (8) (2021) 961–966.
- [13] European Medicines Agency (EMA). RUKOBIA cpr pell ret 600 mg. Summary of the product characteristics. https://www.ema.europa.eu/en/documents/product-information/rukobia-epar-product-information_fr.pdf (accessed 25 October 2022).
- [14] E.B. Chahine, Fostemsavir: The first oral attachment inhibitor for treatment of HIV-1 infection, *Am. J. Health Syst. Pharm.* 78 (2021) 376–388, <https://doi.org/10.1093/ajhp/zxaa416>.
- [15] European Medicines Agency (EMA). Assessment report. Rukobia. https://www.ema.europa.eu/en/documents/assessment-report/rukobia-epar-public-assessment-report_en.pdf (accessed 28 October 2022).
- [16] European Medicines Agency, Guideline on bioanalytical method validation. http://www.ema.europa.eu/docs/en_GB/document_library/Scientific_guideline/2011/08/WC500109686.pdf, 2011 (accessed 11 March 2022).
- [17] U.S. Food and Drug Administration, Guidance for industry: bioanalytical method validation. <https://www.fda.gov/files/drugs/published/Bioanalytical-Method-Validation-Guidance-for-Industry.pdf>, 2018 (accessed 11 March 2022).
- [18] Federal Act on Research Involving Human Beings. Human Research Act, HRA. <https://www.admin.ch/opc/en/classified-compilation/20061313/index.html#a2> (accessed 25 October 2022).
- [19] R. Bonfiglio, R.C. King, T.V. Olah, K. Merkle, The effects of sample preparation methods on the variability of the electrospray ionization response for model drug compounds, *Rapid Commun. Mass Spectrom.* 13 (1999) 1175–1185, [https://doi.org/10.1002/\(sici\)1097-0231\(19990630\)13:12<1175::aid-rcm639>3.0.co;2-0](https://doi.org/10.1002/(sici)1097-0231(19990630)13:12<1175::aid-rcm639>3.0.co;2-0).
- [20] B.K. Matuszewski, M.L. Constanzer, C.M. Chavez-Eng, Strategies for the assessment of matrix effect in quantitative bioanalytical methods based on HPLC-MS/MS, *Anal. Chem.* 75 (2003) 3019–3030, <https://doi.org/10.1021/ac020361s>.
- [21] P. Hubert, J.J. Nguyen-Huu, B. Boulanger, E. Chapuzet, P. Chiap, N. Cohen, P. A. Compagnon, W. Dewé, M. Feinberg, M. Lallier, M. Laurentie, N. Mercier, G. Muzard, C. Nivet, L. Valat, Harmonization of strategies for the validation of quantitative analytical procedures. A SFSTP proposal—Part I, *J. Pharm. Biomed. Anal.* 36 (2004) 579–586, <https://doi.org/10.1016/j.jpba.2004.07.027>.
- [22] E. Chapuzet, N. Mercier, M.C. Laparra, M. Laurentie, J.C. Nivet, Méthodes chromatographiques de dosage dans les milieux biologiques: stratégie de validation. Rapport d'une commission SFSTP, *STP Pharma Sci.* 7 (1997) 169–194.
- [23] B. Boulanger, P. Chiap, W. Dewé, J. Crommen, P. Hubert, An analysis of the SFSTP guide on validation of chromatographic bioanalytical methods: progress and limitations, *J. Pharm. Biomed. Anal.* 32 (2003) 753–765, [https://doi.org/10.1016/S0731-7085\(03\)00182-1](https://doi.org/10.1016/S0731-7085(03)00182-1).
- [24] E. Rozet, A. Ceccato, C. Hubert, E. Ziemons, R. Oprean, S. Rudaz, B. Boulanger, P. Hubert, Analysis of recent pharmaceutical regulatory documents on analytical method validation, *J. Chromatogr. A* 1158 (2007) 111–125, <https://doi.org/10.1016/j.chroma.2007.03.111>.
- [25] E. Rozet, C. Hubert, A. Ceccato, W. Dewé, E. Ziemons, F. Moonen, K. Michail, R. Wintersteiger, B. Strel, B. Boulanger, P. Hubert, Using tolerance intervals in pre-study validation of analytical methods to predict in-study results. The fit-for-future-purpose concept, *J. Chromatogr. A* 1158 (2007) 126–137, <https://doi.org/10.1016/j.chroma.2007.03.102>.
- [26] D. Hoffman, R. Kringle, A total error approach for the validation of quantitative analytical methods, *Pharm. Res.* 24 (2007) 1157–1164, <https://doi.org/10.1007/s11095-007-9242-3>.
- [27] M. Feinberg, Validation of analytical methods based on accuracy profiles, *J. Chromatogr. A* 1158 (2007) 174–183, <https://doi.org/10.1016/j.chroma.2007.02.021>.
- [28] C.T. Viswanathan, S. Bansal, B. Booth, A.J. DeStefano, M.J. Rose, J. Sailstad, V. P. Shah, J.P. Skelly, P.G. Swann, R. Weiner, Quantitative bioanalytical methods validation and implementation: best practices for chromatographic and ligand binding assays, *Pharm. Res.* 24 (2007) 1962–1973, <https://doi.org/10.1007/s11095-007-9291-7>.
- [29] M. Feinberg, B. Boulanger, W. Dewé, P. Hubert, New advances in method validation and measurement uncertainty aimed at improving the quality of chemical data, *Anal. Bioanal. Chem.* 380 (2004) 502–514, <https://doi.org/10.1007/s00216-004-2791-y>.
- [30] A.L. Gassner, J. Schappler, M. Feinberg, S. Rudaz, Derivation of uncertainty functions from validation studies in biological fluids: application to the analysis of caffeine and its major metabolites in human plasma samples, *J. Chromatogr. A* 1353 (2014) 121–130, <https://doi.org/10.1016/j.chroma.2014.05.047>.
- [31] K. Hirayak, D.E. Koren, Fostemsavir: A Novel Attachment Inhibitor for Patients With Multidrug-Resistant HIV-1 Infection, *Ann. Pharmacother.* 55 (6) (2021) 792–797.
- [32] S. Rudaz, M. Feinberg, From method validation to result assessment: established facts and pending questions, *TrAC Trends Anal. Chem.* 105 (2018) 68–74.
- [33] K. Moore, N. Thakkar, M. Magee, H. Sevinsky, B. Vakkalagadda, S. Lubin, C. Llamoso, P. Ackerman, Pharmacokinetics of Temsavir, the Active Moiety of the HIV-1 Attachment Inhibitor Prodrug, Fostemsavir, Coadministered with Cobicistat, Etravirine, Darunavir/Cobicistat, or Darunavir/Ritonavir with or without Etravirine in Healthy Participants, *Antimicrob. Agents Chemother.* 66 (2022), <https://doi.org/10.1128/aac.02251-21.e02251-02221>.
- [34] Fostemsavir PK Fact Sheet. University of Liverpool. Prudced July 2021. https://liverpool-hiv-hep.s3.amazonaws.com/prescribing_resources/pdfs/000/000/217/original/HIV_FactSheet_FTR_2021_Jul.pdf?1632406754 (accessed 24 October 2022).